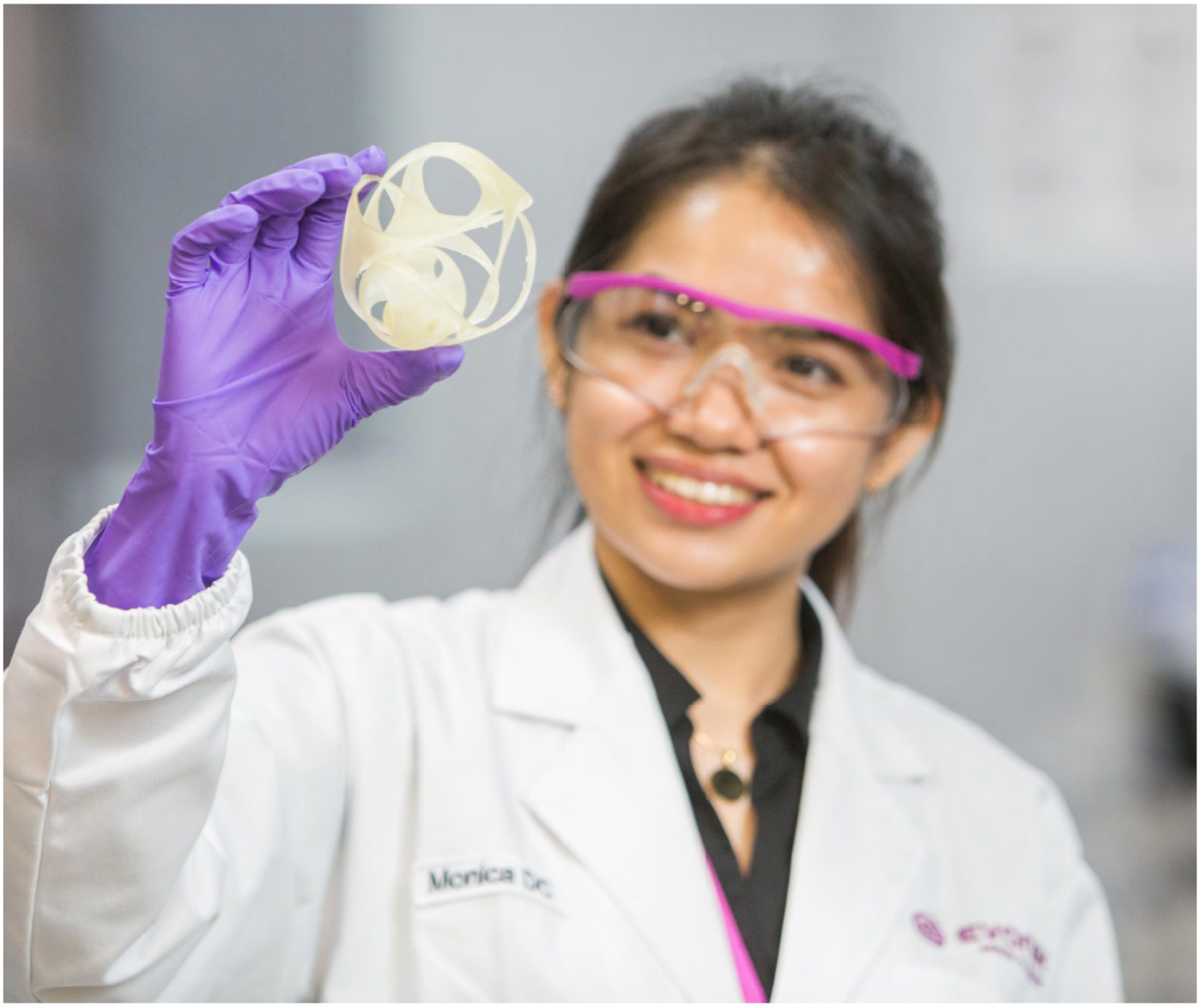

Pushing the boundaries of chemistry? It takes #HumanChemistry

Make your curiosity and talent as a chemist matter to the world with a specialty chemicals leader. Together, we combine cutting-edge science with engineering expertise to create solutions that answer real-world problems. Find out how our approach to technology creates more opportunities for growth, and see what chemistry can do for you at:

evonik.com/career

EVONIK
Leading Beyond Chemistry

ADVANCED FUNCTIONAL MATERIALS
www.afm-journal.de

Tuning the Volume Phase Transition Temperature of Microgels by Light

*Joachim Jelken, Se-Hyeong Jung, Nino Lomadze, Yulia D. Gordievskaya, Elena Yu. Kramarenko, Andrij Pich, and Svetlana Santer**

Temperature-responsive microgels find widespread applications as soft materials for designing actuators in microfluidic systems, as carriers for drug delivery or catalysts, as functional coatings, and as adaptable sensors. The key property is their volume phase transition temperature, which allows for thermally induced reversible swelling/deswelling. It is determined by the gel's chemical structure as well as network topology and cannot be varied easily within one system. Here a paradigm change of this notion by facilitating a light-triggered reversible switching of the microgel volume in the range between 32 and 82 °C is suggested. Photo-sensitivity is introduced by photosensitive azobenzene containing surfactant, which forms a complex with microgels consisting of poly(*N*-isopropylacrylamide-*co*-acrylic acid) (PNIPAM-AAc) chains when assuming a hydrophobic trans-state, and prefers to leave the gel matrix in its cis-state. Using a similar strategy, it is demonstrated that at a fixed temperature, for example, 37 °C, one can reversibly change the microgel radius by a factor of 3 (7–21 µm) by irradiating either with UV (collapsed state) or green light (swollen state). It is envisaged that the possibility to deploy a swift external means of adapting the swelling behavior of microgels may impact and redefine the latter's application across all fields.

1. Introduction

Stimuli responsive microgels consist of cross-linked chains of either homopolymers or co-polymers forming 3D networks, the (chemical) composition of which determines the sensitivity to a certain stimulus.[1–13] For the widely studied poly-*N*-isopropyl acrylamide (PNIPAM) microgels, the volume phase transition, that is, the swelling/growth or deswelling/shrinkage along with expelling or absorbing water can be toggled by an appropriate change in temperature around the so-called volume phase transition temperature (VPTT) of 32 °C, due to the presence of both hydrophilic amide groups and hydrophobic isopropyl groups in the interior.[14–20] Introducing acid or base groups into polymer chains makes the microgels additionally responsive to changes in pH or ionic strength.[21–28] Moreover, the charged groups significantly alter the VPTT causing it to shift towards larger values.[29–33] The temperature-induced swelling/deswelling transition is determined by the counterbalance of the hydrophobic attraction of NIPAM groups at elevated temperatures and the osmotic pressure of the counter-ions trapped within the particle as well as repulsive electrostatic interactions of the network charges. A maximal temperature shift up to 63 °C has been reported for a microgel with linear grafted poly(NIPAM-co-AAc) side chains ≈20 mol% of acrylic acid (AAc) groups.[34]

One should emphasize that the above-mentioned flexibility in shifting the VPTT is related to changing the chemical composition of polymer chains or the environment of the microgel network, such that a simple reversible switching of microgel size is precluded.

However, the charged groups also allow for complexation with oppositely charged ions or small molecules. Employing an

J. Jelken, N. Lomadze, S. Santer
Institute of Physics and Astronomy
University of Potsdam
14476 Potsdam, Germany
E-mail: santer@uni-potsdam.de

S.-H. Jung, A. Pich
DWI-Leibniz Institute for Interactive Materials e.V
52074 Aachen, Germany

S.-H. Jung, A. Pich
Functional and Interactive Polymers
Institute of Technical and Macromolecular Chemistry
RWTH Aachen University
52074 Aachen, Germany

Yu. D. Gordievskaya, E. Yu. Kramarenko
Faculty of Physics
Lomonosov Moscow State University
Moscow 119991, Russia

Yu. D. Gordievskaya, E. Yu. Kramarenko
A. N. Nesmeyanov Institute of Organoelement Compounds RAS
Moscow 119991, Russia

A. Pich
Aachen Maastricht Institute for Biobased Materials (AMIBM)
Maastricht University
Geleen 6167 RD, The Netherlands

The ORCID identification number(s) for the author(s) of this article can be found under https://doi.org/10.1002/adfm.202107946.

DOI: 10.1002/adfm.202107946

azo-containing cationic surfactant for this purpose, photosensitivity can be introduced, which leads to an intriguing phenomenology.[35] For instance, the swelling degree of microgel can be reversibly changed between the collapsed and the swollen state simply using an appropriate optical stimulus triggering *trans-cis* isomerization.[36] Depending on the surfactant concentration added to the microgel we can distinguish two regions where the swelling can be induced upon illumination with UV light (low concentration region, Region I) or green/blue light (above critical micelle concentration (CMC), Region II).[37] While the shrinkage is achieved on irradiation with green/blue light (Region I) and with UV (Region II). The up to eightfold change in volume is completely reversible. In the theory proposed we explain the photo-triggered behavior of the photo-sensitive microgel in Region I with the behavior of osmotic pressure within the particle interior during reversible absorption and desorption of the two different azobenzene isomers, namely, the surfactant in the *trans*-state is preferentially absorbed by the microgel, while in the *cis*-state it prefers to stay in water, because along with the change in the azo component, the physico-chemical properties of the surfactant as a whole change, such as its hydrophobicity conveyed by the polarity of incorporated hydrophobic tail.[38,39] Hence, the surfactant molecule in its *trans*-state is more hydrophobic with a corresponding low CMC, while the *cis*-conformation results in more hydrophilic state with an up to tenfold increase of the CMC. This aspect unique to azobenzene-containing surfactant can further be exploited, for instance, to change interaction strength with other substances and allows for diverse applications such as light triggered compaction/decompaction of DNA molecules,[40–44] reversible and irreversible structuring of polymer films,[45–47] control of hydrodynamic flows at water/air and solid/water interfaces.[48–59] The key aspect for microgel matrices is that osmotic pressure can be changed reversibly, conveyed by the remarkable control that can be attained over whether a surfactant molecule leaves or stays with the microgel matrix. This is at variance with other conceivable ions or charged molecules that might have been taken into consideration as well. At higher surfactant concentrations, well above the CMC, where electrostatics is largely screened, another effect can come into play, namely, a preferable solubilization of hydrophobic PNIPAM subchains by *trans*-isomer micelles favoring microgel swelling and shifting VPTT to higher temperatures. An increase of globule-to-coil transition temperature of PNIPAM with an increasing surfactant concentration has previously been reported in Refs. [60–62]. Using light as the trigger of surfactant hydrophobicity, it becomes possible to control the degree of surfactant-microgel complexation and to tune the VPTT at high surfactant concentrations as well.

Here we show experimentally and theoretically that above-mentioned phenomenology can be exploited to swiftly tune the VPTT over a surprisingly broad range using light as a stimulus. This temperature, which for a polymer is also referred to as the lower critical solution temperature, is the only other external control parameter that can be used to trigger swelling/deswelling without chemically changing the microgel in a single closed system. Using light to modulate the VPTT of microgels offers numerous advantages compared to other stimuli like temporal and spatial control and exogenous application. In addition, the application of different molecular photo-switches allows modular design of microgels able to respond to light of specific wavelengths. With this additional control knob, we expect that many applications where microgels are in use can be revisited or optimized, or additional applications previously impractical can be devised.

2. Experimental Section

NIPAM (*N*-Isopropylacrylamide, 97%, recrystallized), AAc (Acrylic acid, 99%, anhydrous, contains 200 ppm MEHQ as inhibitor, filtered in column with silica filled), BIS (*N*,*N*′-Methylenbis(acrylamide), 99%), APS (Ammonium persulfate, ≥98%), span 80, 1.4-dioxane (≥99%), TEMED (*N*,*N*,*N*′,*N*′-tetramethyl ethylenediamine, 99%) were obtained from Sima-Aldrich. Isopropanol (≥99.6%) and hexane (≥98.5%) were obtained from VWR. PDMS kit (Sylgard 184) was purchased from Downsil. HFE (Novec 7500) was provided by 3M. Krytox FSH was obtained from Chemours.

2.1. Synthesis of Poly(NIPAM-co-AAc) Microgels using Microfluidics

Microgels were prepared utilizing free-radical polymerization in a droplet-based microfluidic by varying monomer (NIPAM) and comonomer (AAc) concentrations. The sum of monomer and comonomer concentrations are 0.83 mg L^{-1}, 100 mol%. NIPAM (100 to 80 mol%), acrylic acid (0 to 20 mol%), BIS (3.4 mg, 0.02 mmol, 2.5 mol % based on monomer concentrations), APS (10 mg) were dissolved in water (1 mL). The mixture was degassed under Ar for 5 min. and transferred into glass syringes. At the cross-junction of the PDMS device, water-in-oil droplets were formed by flow-focusing of the water phase exerted by the oil phase. For the continuous phase, fluorocarbon oil (HFE-7500) containing 1.8 vol% of Krytox FSH and 2 vol% of TEMED was used. The following volume flow rates were applied to generate emulsions w/o: water phase (dispersed phase): 50 µL h^{-1}, oil phase (continuous phase): 60 µL h^{-1}. Droplets were collected in 2 mL of vials for 4 h and were allowed to react overnight at room temperature. Afterward, the fluorocarbon oil was removed, and the obtained microgel particles were washed with different solvents. Between washing steps, the microgels were allowed to sediment or float on the solvent followed by replacement by fresh solvents. The procedure was performed with plain HFE-7500 three times, with hexane containing 1 wt% span 80 one time, with hexane three times, with isopropanol three times (with centrifuge 5000 rpm for 10 min), with 1, 4 dioxane three times (with centrifuge 5000 rpm for 10 min) and with water (MiliQ) three times (with centrifuge 8000 rpm for 10 min). Finally, microgels were re-dispersed in fresh water.

2.2. Device Fabrication

Microfluidic devices were fabricated by soft lithography. AutoCAD (Autodesk, USA) software was used to design the microfluidic channel in a 2D drawing, which was printed on a high-resolution (25.000 dpi) dark-field photomask.

Photolithography was applied to pattern an epoxy-based photoresist (SU-8) on a silicon wafer using the printed photomask as template. PDMS along with crosslinker (Silgard 184 elastomer kit, Dow Corning, USA, base: crosslinker = 10:1) was poured on the previously prepared silicon wafer and excess of air was removed under high vacuum for 30 min. The mixture was solidified at 65 °C overnight (12 h). The cured PDMS mold was peeled off from the silicon wafer and washed with isopropanol and water three times. The devices were fabricated by oxygen plasma (100 W, 40 s) bonding of the PDMS replicas onto glass slides. The device was heated at 120 °C, 5 min for total completion of the bonding and evaporating water generated from the condensation reaction. After finalization of the bonding process of the PDMS mold to the glass slide, the silane solution Aquapel (Pittsburgh Glass Works, USA) was used to render the microfluidic channels hydrophobic by 50 mL syringes. The residual silane solution was removed by plain fluorocarbon oil (HFE-7500) using another 50 mL syringe.

2.3. General Workflow for Microfluidic Devices

Microfluidic experiments were conducted on a microfluidic system consisting of two syringe pumps (PHD Ultra, Harvard Apparatus, Holiston, USA), to control the flow rates of the two different phases. An inverted microscope (Motic AE2000, TED PELLA, INC., Redding, CA) equipped with a camera (Flea3, Point Grey, Richmond, CA) was applied to observe flow and droplet formation. The PDMS microfluidic device was connected to the system using fine bore polyethylene tubing (0.86 mm inner diameter, 1.52 mm outer diameter, VWR). The microchannels have a rectangular cross-section with a uniform height of 20 µm.

2.4. Light Responsive Surfactant

The surfactant molecule (**Figure 1**a) consists of a cationic trimethylammonium bromide head group connected via a spacer of 6 methylene groups to the azobenzene unit with butyl tail attached.[33] A stock solution of surfactant was adjusted to the concentration of 10 mM and diluted to the required concentrations.

2.5. Optical Properties of the Surfactant

The photo-isomerization of the surfactant was described elsewhere.[63] For short, the *trans* isomer has a characteristic absorption band (π–π^* transition) with a maximum at 351 nm. Under UV illumination at 365 nm, at photo-stationary state, there were 10% of *trans*- and 90% of *cis*-isomers. The spectrum of the *cis* isomer was characterized by two absorption bands with maxima at 313 nm (π–π^* transition) and at 437 nm (n–π^* transition). Under irradiation with green light (λ = 532 nm), the majority of the surfactant was in *trans* state with the *trans/cis* ratio of 90/10%. The photo-isomerization was intensity-dependent above CMC (0.5 mM for *trans*-isomer) and takes place within seconds.

2.6. Optical Setup and Data Analysis

An Olympus microscope IX73 equipped with commercial multiple monochromatic LED light source (Thorlabs, for UV, λ = 365 nm, M365 LP1; for green, λ = 530 nm, M530 L2-C1; for red, λ = 625 nm, M625 L2-C) acts as illumination and monitoring source. The intensity of all LED lamps is set to 1 mW cm^{-2}. Images were monitored with Hamamatsu Camera ORCA-Flash 4.0 LT at a monitoring speed of 1 frame per second. Samples were kept in dark to prevent uncontrolled isomerization.

Time-resolved diameter change of the microgels was acquired under illumination from top with monochromatic light of λ = 625 nm (red) and was analyzed using the software Image J by calculating for each frame the area occupied by particle.

2.7. Temperature

Temperature was controlled by a homemade heating stage, where an indium tin oxide (ITO) coated glass slide was

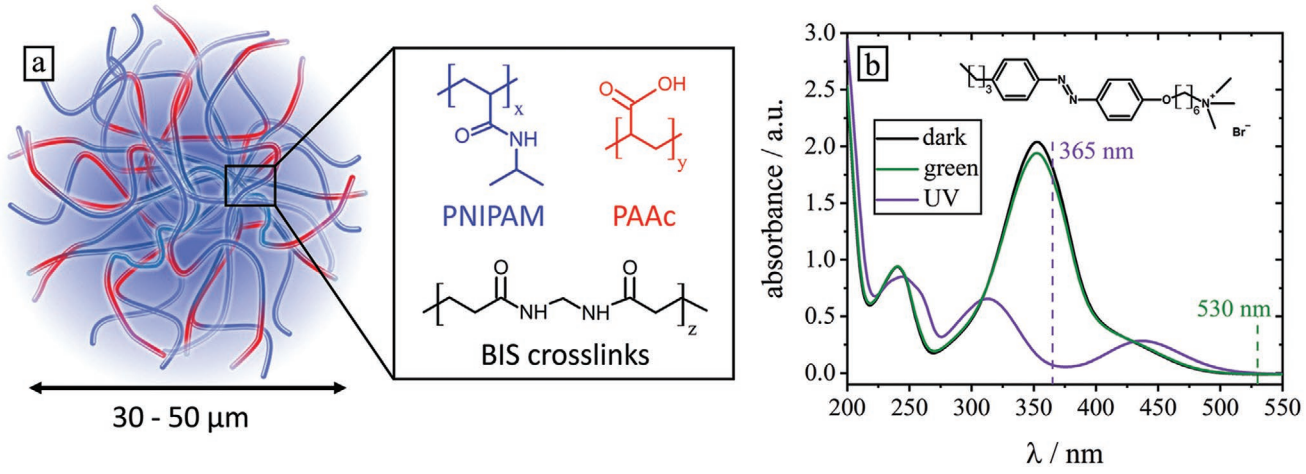

Figure 1. a) Scheme and chemical structure of the microgel. b) Chemical structure of the azobenzene-containing surfactant and its UV–Vis adsorption spectra.

equipped with two silver electrodes. The ITO layer was facing towards the objective and isolated from the microscope stage. Applying a voltage to the electrodes (max. 30 V) was heating up the glass slide to max. 100 °C. The temperature was measured with a PT100 resistance thermometer attached to the glass side. The rate of temperature change is kept as 1 °C per 10 s.

3. Theory

The microgel is considered to consist of ν flexible subchains each containing N monomer units. Some fraction f of the monomer units is ionic. According to the experimental system, the microgel subchains are negatively charged while the counterion charges are positive. To describe changes in the microgel volume, it is useful to introduce dimensionless swelling ratio $\alpha = R/R_0$, which is the ratio between the equilibrium microgel radius R, and the microgel radius R_0 in the reference state. The reference state corresponds to the network with Gaussian subchains, $R_0 = aN^{1/2}\ \nu^{1/3}$, a being a monomer unit size. The average distance between the centers of adjacent microgels in the solution is established as $2R_{out} = 2R_0/\gamma$ with the dimensionless parameter γ defined by microgel concentration, $\gamma \ll 1$ for dilute solutions.

We denote as Z the number of surfactant molecules in the solution per one charged group on polymer subchains. Salt-free case is considered, that is the counterions of the microgel particles, surfactant ions, and surfactant counterions are the only mobile ions in the system. We use the two-zone model to account for the redistribution of ions between the microgel interior and the outer solution,[37,38] resulting in an uncompensated microgel charge of $Q/e = \nu Nf(\beta - 1 + sZ - tZ)$, where e is the elementary charge while s, β, and t denote the total fractions of surfactant molecules, network counterions, and surfactant counterions, respectively, that are kept within the microgel. It is known that the critical aggregation concentration of surfactants in microgels is much less than solution CMC due to micelle charge neutralization by ions on gel subchains, so that micelle formation inside microgels starts at very low surfactant concentrations.[36–38] We consider the general case when the charge of micelles with the aggregation number m is partly neutralized by both oppositely charged monomer units and by surfactant counterions. Counterion immobilization in the vicinity of micelles is important when the total charge of the microgel is close to zero, this situation is realized at surfactant concentrations close to and above CMC. Accordingly, Coulomb energy of the charged micelles and losses in the translational entropy of surfactant counterions should be taken into account in the total free energy of the microgel solution.[38]

Thus, the free energy of the solution per microgel is given by:

$$F_{tot} = F_{el} + F_{int} + F_{el-st} + F_{el-st}^{mic} + F_{tr}^{nc} + F_{tr}^{sc} + F_{tr}^{s} + F_{agg} \quad (1)$$

The first term is the energy of elastic deformation of the microgel subchains

$$\frac{F_{el}}{k_B T} = \frac{3}{2}\nu\left(\alpha^2 + \frac{1}{\alpha^2}\right) \quad (2)$$

The contribution from volume interactions of microgel monomer units, F_{int}, is written in the Flory–Huggins form:

$$\frac{F_{int}}{k_B T} = \left(\frac{R}{a}\right)^3\left[(1-\Phi)\ln(1-\Phi) - \left(\chi + \Delta\chi\frac{ZN\nu fsq/m}{\nu}\right)\Phi^2\right] \quad (3)$$

where $\Phi = \nu Na^3/R^3$ is the polymer volume fraction inside the microgel, χ is the Flory–Huggins parameter for monomers units of the microgel. Changes in solvent quality, which are experimentally realized by variation of temperature, are described by varying χ-parameter in the theory. The parameter $\Delta\chi$ is introduced to describe increasing solubility of microgel subchains due to adsorption of micelles from *trans*-isomers, $\frac{ZN\nu fsq/m}{\nu}$ is the number of micelles per one subchain. At low surfactant concentrations, the contribution from $\Delta\chi$ term is negligible. However, at high surfactant concentrations well above CMC, the hydrophobic interactions between non-ionic polymer units and hydrophobic tails of surfactant molecules give significant contributions to the free energy because the fraction of the surfactant phase inside microgels becomes comparable with the polymer volume fraction. It has previously been shown that indeed polymer-surfactant complexation can cause a globule to coil transition.[65] In calculations, we put $\Delta\chi = 0.4 - \chi$ for *trans*-isomers. It is assumed that *cis*-isomers do not interact with monomer units, for them $\Delta\chi = 0$.

The next term, $F_{el\ -\ st}$, accounts for the excess Coulomb energy of the charged microgel and the outer solution, treated as the energy of a spherical capacitor with R and R_{out} as the radii of the internal and the external plates, respectively:

$$\frac{F_{el-st}}{k_B T} = \frac{Q^2}{\varepsilon k_B T}\left(\frac{1}{R} - \frac{1}{R_{out}}\right) \quad (4)$$

where ε is the relative dielectric permittivity of the solvent.

The Coulomb energy of the charged micelles, F_{el-st}^{mic}, is taken into account within the same approach:

$$\frac{F_{el-st}^{mic}}{k_B T} = N_{mic}\frac{Q_{mic}^2}{\varepsilon k_B T}\left(\frac{1}{R_{mic}} - \frac{1}{R_{out}^{mic}}\right) \quad (5)$$

where $N_{mic} = \frac{N\nu fZsq}{m}$, $R_{mic} = (mb^3a^3)^{1/3}$ and $Q_{mic} = e\left(1 - \frac{1+Ztd}{Zsq}\right)m$ are the number of micelles, radius, and charge of micelles, respectively, ba being a surfactant size. $2R_{out}^{mic}$ is the average distance between micelles. We consider the polyelectrolyte regime, assuming $e^2/\varepsilon a k_B T = 1$. At high surfactant concentrations, well above the CMC, electrostatic interactions are screened by surfactants and surfactant counterions (high salt regime) and the electrostatic contributions to the free energy, $F_{el-st} + F_{el-st}^{mic}$, are negligible.

The terms F_{tr}^{nc} and F_{tr}^{sc} are responsible for the translational entropy of the microgel and the surfactant counterions, which are regarded as an ideal gas both inside and outside the microgel:

$$\frac{F_{tr}^{nc}}{k_B T} = fN\nu\left[\beta \ln\left(\beta f \Phi\right) + (1-\beta)\ln\left(\frac{(1-\beta) f \Phi \gamma^3}{\Phi N^{1/2} - \gamma^3}\right)\right] \quad (6)$$

$$\frac{F_{tr}^{sc}}{k_B T} = ZfN\nu\left[\begin{array}{c} t(1-d)\ln\left(Zt(1-d) f \Phi\right) + td\left(\frac{N\nu Ztdf}{S_{mic} a}\right) \\ +(1-t)\ln\left(\frac{Z(1-t) f \Phi \gamma^3}{\Phi N^{1/2} - \gamma^3}\right) \end{array}\right] \quad (7)$$

We assume, that the fraction d *of* the condensed surfactant counterions are able to move in the outer layer of micelles total area $S_{mic} = R_{mic}^2 N_{mic} = N\nu fZsqb^2$.

The term F_{agg} accounts for the micelle formation inside microgels. If q is the fraction of surfactants aggregated into micelles, the aggregation energy F_{agg} can be written as:[38]

$$\frac{F_{agg}}{k_B T} = N\nu Zfs\left[\begin{array}{c} (1-q)\ \ln(1-q) + \frac{q}{m}\ \ln(q) - q\frac{m-1}{m}\ln\left(\frac{Zsf\Phi}{e}\right) \\ -q\Delta F\left(1 + \frac{k_1}{e^{\left(\frac{ZN\nu fsq/m}{\nu} - \frac{1}{2}\right)k_2} + 1}\right) \end{array}\right] \quad (8)$$

where ΔF is the energy gain per surfactant ion due to micellization in solution and the last term in the last brackets accounts for its variation for mixed micelles which are mainly formed inside microgels at high surfactant concentrations and contain some fraction of hydrophobic subchains of microgels. The more micelles per subchain are formed inside microgels the smaller gain from micellization. The parameters k_1 and k_2 regulate the effect of the hydrophobic environment of surfactant molecules within microgels, their values are chosen to equal $k_1 = 0.05$ and $k_2 = 3$ to better reproduce the experimental data. At low surfactant concentrations, this correction to the energy gain is negligible.

Translational entropy of non-aggregated surfactant ions both inside and outside the microgel is taken into account by the term F_{tr}^{sc} which reads

$$\frac{F_{tr}^{sc}}{k_B T} = ZfN\nu\left[s\ln\left(Zsf\Phi\right) + (1-s)\ln\left(\frac{Z(1-s) f \Phi \gamma^3}{\left(\Phi N^{1/2} - \gamma^3\right)}\right)\right] \quad (9)$$

When the surfactant concentration exceeds CMC, micelle formation is also realized outside the microgel, this fact is taken into account via additional contribution to the free energy, F_{agg}^{out},

$$F_{agg}^{out} = N\nu Zf(1-s)\left[\begin{array}{c} (1-r)\ \ln(1-r) + \frac{r}{m}\ \ln(r) \\ -r\frac{m-1}{m}\ln\left(\frac{Z(1-s) f \Phi \gamma^3}{\exp\left(\Phi N^{1/2} - \gamma^3\right)}\right) - r\Delta F \end{array}\right] \quad (10)$$

where r is fraction of associated surfactants outside the microgel. This term is zero below CMC.

The free energy is minimized according to equilibrium conditions, that is, equality of osmotic pressure as well as equality of chemical potentials of all ionic species inside and outside microgels.

The values of the main parameters describing microgel particles as well as the concentration of microgels in the solutions are chosen in accordance with experimental systems: = 10^8, N = 50, f = 0.1, γ = 0.1, these values are fixed in all calculations. The aggregation number, m, of micelles formed by the surfactants both in *trans*- and *cis*-states is taken equal to 50, which is known to be typical aggregation number of spherical micelles. In fact, the exact numerical value of $m \gg 1$ hardly influences theoretical conclusions. To account for a higher hydrophobicity of surfactants in *trans*-state, we put the values of the energy gain from micellization equal to ΔF = 10 and ΔF = 7 for *trans*- and *cis*-isomers, respectively. The proposed model explains the conformational behavior of microgels in a solution of photosensitive surfactants, and the obtained theoretical dependences qualitatively agree with the experimental data, as it will be shown below.

4. Results and Discussion

We study microgels differing in the amount of AAc groups integrated within the network: 0% (pure PNIPAM), 1 mol%, 3, 5, 10, and 20 mol% (Figure 1a). Considering the synthesis method, the crosslinked PNIPAM polymer chains within microgel network contain randomly distributed AAc units. The VPTT point of synthesized microgels shifts towards larger temperature with increasing the amount of charged group (measurements performed at neutral pH) (**Figure 2**). The maximal transition temperature is found for the 20 mol% of AAc groups to be 72 °C. The initial size of the microgel depends on the AAc content as well (see Figure 2a at room temperature), so that the pure PNIPAM microgel has radius of 14 μm while the mostly swollen is the 20 mol% AAc microgel with the radius of 28 μm.

The increase of the VPTT, as well as the increase in the initial size of the microgel, is associated with the enhanced osmotic pressure within the particle due to the presence of the counterions and the additional electrostatic repulsion of the network charges.[29–33]

On adding surfactant molecules, they diffuse in the *trans*-state within the microgel and form micelles at concentrations much lower than the bulk CMC. The process governed by the entropy gain of water molecules on micellization as well as less entropy drop on neutralization of the micelle surface charge by the network charges since they are intrinsically pure of entropy due to binding to the polymer chains compared to freely moving counter-ions.[64] The complexation of the surfactant with the AAc groups of microgel network alters the VPTT significantly (**Figure 3**).

With the 5 mol% AAc microgel, we demonstrate that the VPTT point depends strongly on surfactant concentration. On adding of small amount of surfactant the VPTT point shifts from 50 °C in pure water to 32 °C (Region I in Figure 3a), at the concentration range between 0.1 mM and ≈0.5 mM the VPTT point is at 32 °C due to compensation of the network charges (Figure 3a). In this range, the microgel size drops down two times. This is explained by the osmotic pressure drop since due

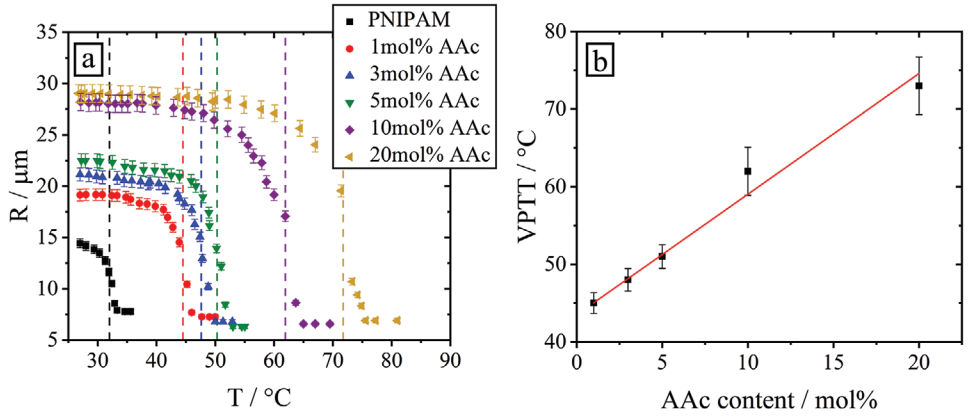

Figure 2. a) Dependence of the microgel size on the temperature for 6 particles differing in the amount of acryl acid (AAc) groups: pure NIPAM (black points), 1 mol% (red points), 3 mol% (blue points), 5 mol% (green points), 10 mol% (purple points), 20 mol% (yellow points). b) Dependence of the VPTT on the amount of the integrated AAc groups. The VPTT increases consequently from 32 °C up to 72 °C with increasing the AAc amount from 0% to 20 mol%.

to electro-neutrality principle the natural counter-ions of the gel are expelled out when the surfactant enters the interior.[64] With further increase of the surfactant concentration the VPTT shifts towards larger values accompanied by the increase of the microgel size. This behavior we explain by screening of hydrophobic interactions of microgel subchains by surfactant micelles. The intramolecular solubilization causes microgel swelling similar to the globule-to-coil transition and swelling of PNIPAM chains in surfactant solutions reported in Refs. [60–62].

Solubilization of microgels by surfactants may shift the VPTT to higher values compared to the VPTT of microgel in pure water. Indeed, in the case of 10 mol% AAc gel, the VPTT point is at 62 °C in water, but can be tuned to ≈80 °C at surfactant concentration of 10 mM (Figure 6e). In the case of 20 mol% at concentration of 10 mM, the VPTT point shifts towards 95 °C. The optical visualization of the microgels at such high temperatures is difficult due to significant fluctuation in the reflective index of water as well as fast evaporation of the solvent even in tightly closed samples. Therefore, we report here on comprehensive study of the microgels up to 10 mol% in the broad concentration region of the surfactant. A series of measurements for the highly charged microgels (20 mol% AAc) is also conducted, however, avoiding range of VPTT points above 70 °C (Figure S1, Supporting Information).

Photo-responsiveness of the azobenzene-containing surfactant allows for the light triggered reversible switching of the microgel size as reported by our group recently.[35] Here there are two regions of different response of microgel on irradiation with light of two distinct wavelength (Figure 3b). In general, the *trans*-isomer (green light, λ = 530 nm) prefers to state in the pores of the microgel, while the less hydrophobic *cis*-isomer (blue light, λ = 365 nm) diffuses out. This defines the mechanism of the remote control of the microgels size by light.[35] In Region I, the *trans*-isomers replace native counter-ions of the gel causing osmotic pressure drop and collapse, while under irradiation with UV light the *cis*-molecules leave the particle and the microgel swells again. In Region II, the opposite behavior is observed: the microgel swells on irradiation with green light (λ = 530 nm, *trans*-state) due to over-charging and additional trapping of the surfactant counter-ions in the gel; but

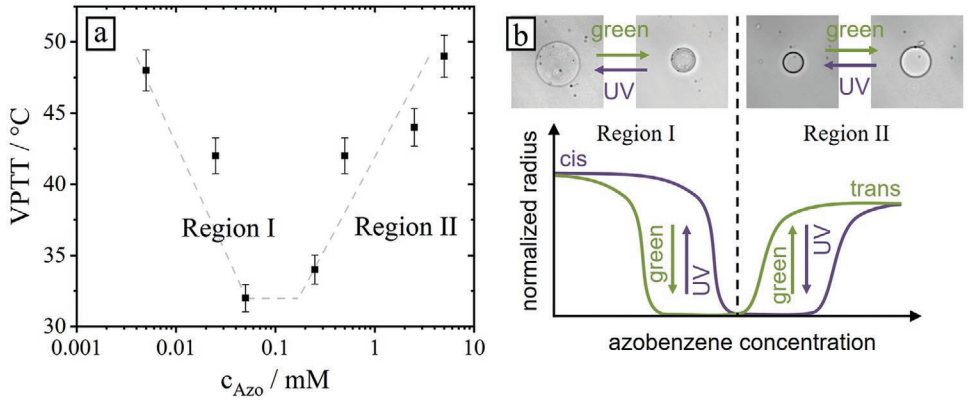

Figure 3. a) Dependence of the VPTT point on surfactant concentration illustrated for the microgel with 5 mol% AAc. The measurements are performed at neutral pH. b) Dependence of the microgel size on surfactant concentration plotted for two states of the azobenzene *trans* (green curve) and *cis* (blue curve) at room temperature.[26] In Region I, on irradiation with UV light the microgel swells, while in Region II where the microgel is overcharged it results in shrinking. Above the corresponding optical micrographs of the microgel under irradiation with different wavelength are depicted.

shrinks during exposure to UV light (λ = 365 nm, *cis*-enriched state) (Figure 3b). The change in radius during photo-triggered switching between swollen and shrunk state is two times for both regions. We should emphasize that the volume phase transition triggered by light takes place at a fixed absolute concentration of the surfactant. Depending on the response needed, that is, swelling or shrinkage on irradiation with light, one can just choose the initial absolute concentration (see Figure 3b) and then change the volume of the microgel just by varying the wavelength of applied irradiation. During light-induced swelling/shrinkage of the microgel, the surfactant molecules either diffuse in or out, that is, the amount of the stored surfactant within the gel is varied, and thus its overall charge can be tuned. Therefore, the irradiation alters the VPTT point significantly as well.

Let's first discuss the Region I of low surfactant concentrations (**Figure 4**a). Here the microgel is in collapsed state in dark with the radius of 12 µm at room temperature (a majority of surfactant is in *trans*-state) (black points in Figure 4a). With increasing the temperature the microgel radius drops down to 7 µm, the transition is continuous, that is, starts at 29 °C and saturates at 36 °C, defying the VPTT point at ≈32 °C. When, however, the microgel is irradiated with UV light at room temperature the radius increases to 24 µm (violet points in Figure 4a), and with temperature increase drops down to 7 µm at ≈39 °C. After cooling down, under irradiation with green light (blue points in Figure 4a), the VPTT shifts again to 32 °C. Similar response but with orthogonal stimuli, that is, VPTT is at 32 °C under UV light, and shifts to ≈50 °C in dark, is observed for the Region II (Figure 4b). Remarkably, that for both concentration regions, at any fixed temperature, one can change the microgel size reversible by light. For instance, when we keep the temperature at 36.6 °C (Figure 4b) in Region II under UV light the microgel is in collapsed state with 7 µm radius, but on changing the wavelength to green λ = 532 nm, the particle swell immediately within 10 s to 18 µm. The same is true for the Region I, here one can get the maximal change in the size at 36.6 °C: under green light (d = 7 µm) and under UV light (d = 21 µm) implying 27 times change in the volume (Figure 4a). Both processes of temperature and light-induced volume phase transition are fully reversible and can be repeated many times. Theoretically, we show that in the case of low surfactant concentration micelle formation inside the gel occurs due to the gain in translational entropy of counterions: the charged surfactants are partially neutralized by oppositely charged units of the microgel, there are fewer losses in the translational entropy of surfactant counterions. And since the hydrophobicity of the *trans*-isomer tails is greater, aggregation within the gel takes place at lower surfactant concentrations and at a better solvent quality for the

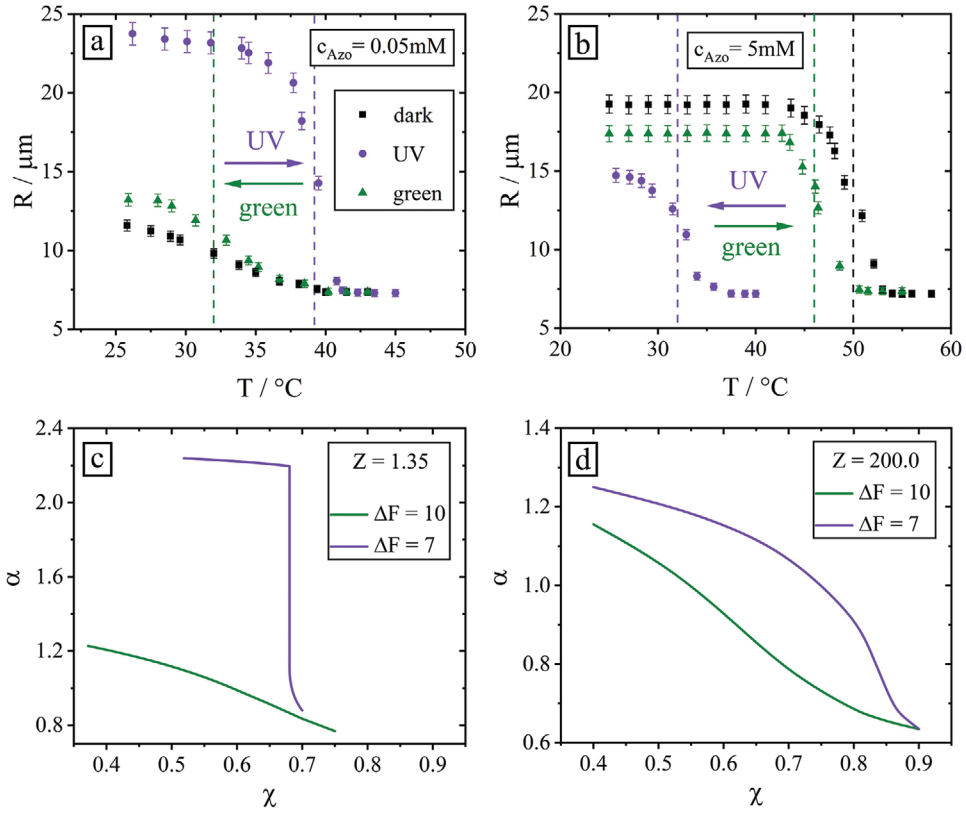

Figure 4. Dependence of the microgel size (5 mol% AAc) on the temperature during irradiation with light of different wavelength: green light, λ = 530 nm (green points), relaxed state with 100% of *trans*-isomers (black points) and under irradiation with UV light λ = 365 nm (violet points) at two different surfactant concentrations a) c = 0.1 mM (Region I) and b) c = 10 mM (Region II). All measurements are performed at neutral pH. The corresponding videos are provided in Integrated Multimedia. c,d) Theoretically calculated swelling ratio of the microgel as a function of the Flory–Huggins parameter for polymer, χ, at different amount, Z, of *trans*- (green curves) and *cis*- (violet curves) isomers: c) Z = 1.35, d) Z = 200.

polymer (lower χ in the theory and temperature in the experiment, Figures 4a–c). The addition of a large number of charged surfactant leads to salting and a decrease in the strength of electrostatic interactions. Here, the main factor is the hydrophobic interaction of the surfactant tails and monomer units of the gel. Since the *trans*-isomers are highly hydrophobic and they tend to bind to hydrophobic objects (nanoparticles, polymers), they interact with the monomer units improving the solubility of the subchains in the solvent. In the system with molecules in the *cis*-state, the conformational behavior of a microgel is similar to that of a neutral macrogel (Figures 4b-d).

Figure 5 summarizes schematically the process of multiple response of the dual thermo-photo-sensitive microgels over surfactant concentration range between 0.1 and 10 mM for AAc 5 mol%.

The same tendency is observed for all microgels studied here with corresponding shift in the concentration range defining the Regions I and II (**Figure 6** shows example for 10 mol% AAc gel). Here, for example, at 42 °C one can change the size of the gel between 7 µm (green light) and 22 µm (UV light) implying ≈30 times change in the particle volume (Figure 6f). The maximum change in the transition temperature of ΔT = 50 °C is found for 10 mol% microgel, where one can switch by light the VPTT point between 32 °C under UV and 82 °C under green irradiation (Figure 6e). At surfactant concentration of 0.25 mM (Figure 6b) the microgel does not show photo-responsivity, since it corresponds to the transition between two regions (see scheme in Figure 3b), where the charge compensation of the gel exists for both isomers, *trans* and *cis*. This also influences the change in the size under temperature increase, that is, the volume phase transition is continuously taking place over ≈20 °C range (Figure 6b). Theoretically calculated curves of these systems match very well the experimental results as shown in Figure S2, Supporting Information.

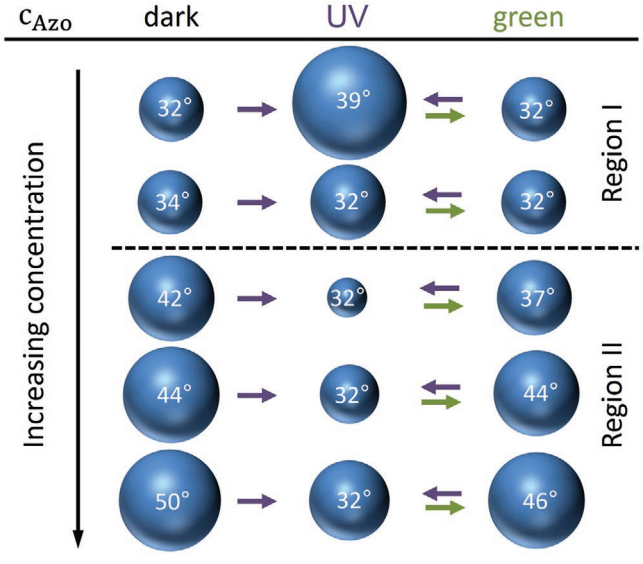

Figure 5. Scheme relating VPTT point (shown in white on microgels in blue) and the size of the 5 mol% AAc microgel to different surfactant concentrations (y-axis) and irradiation wavelength (x-axis).

We should mention that in the absence of the surfactant, the VPTT of microgels is altered by the presence of additional ions, such as sodium chloride or sodium hydroxide. For instance, the transition temperature is shifted from 50 °C in pure water to 55 °C at 10 mM NaCl (pH = 7) and 10 mM NaOH (pH = 12) (see Figure S3, Supporting Information). However, the added surfactant molecules replace the counter-ions within the gel and recover the photo-sensitivity of the PVTT (Figure S4, Supporting Information).

Interestingly, for different surfactant concentration regions, microgels exhibit different shapes upon shrinkage induced by temperature increase. Indeed, for the case when the microgel is already in a compact state due to surfactant absorption, the temperature-induced deswelling leads to the reduction of the microgel size, but the spherical shape of microgels is preserved at all temperatures (see for example **Figure 7**a).

In case when the microgel is in a swollen state, which is possible in three situations (below PVTT): in water without added surfactant (see typical example in Figure 7c), in dark in the Region II (for instance see video in Integrated Multimedia) or under UV light in the Region I (see Figure 7b as an example), the temperature-induced change in size is steeper and accompanied by inhomogeneous shrinkage. There are areas on the microgels, which shrink first resulting in constriction shape of the particles (Figures 7b,c) followed by continuous blowing off. This effect may originate from the heterogeneity of the polymer network, which induces nano-phase separation within microgel under temperature increase due to local enrichment of the microgel interior with only PNIPAM-rich or AAc-rich chain segments and their shifted temperature response. So that the PNIPAM-rich segments shrink first inducing backlink instability of the elastic body under changing osmotic pressure. During microgel swelling induced by either cooling or at fixed temperature by irradiation, the shape change is recurred in reverse manner as can be seen in videos (see videos related to Figure 7).

5. Conclusion

In this work, we have introduced for the first-time light-driven remote control of VPTT of microgels over broad range of temperatures, that is, between 32 °C and up to 95 °C. We support our finding by theoretical calculations covering a wide range of surfactant concentrations and solvent quality and discuss the mechanism of light-triggered VPTT shift.

The microgels consist of crosslinked temperature- and pH-responsive poly(*N*-isopropylacrylamide-co-acrylic acid) p(NIPAM-AAc) chains with variable acrylic acid (AAc) contents ranging between 0 and 20 mol%. The presence of the negative charges within the microgel due to dissociation of the carboxylic groups of the AAc alters the size of the microgel as well as the VPTT point significantly. Thus, the radius of the microgels dispersed in water at room temperature increases from 14 µm (PNIPAM) to 28 µm (p(NIPAM-AAc-20 mol%)) with corresponding shift of the VPTT point from 32 to 72 °C. The VPTT point is also altered by the amount of added oppositely charged surfactant due to charge compensation and solubilization of microgel subchain by surfactant micelles. In the latter case, the VPTT point approaches that one as in pure water

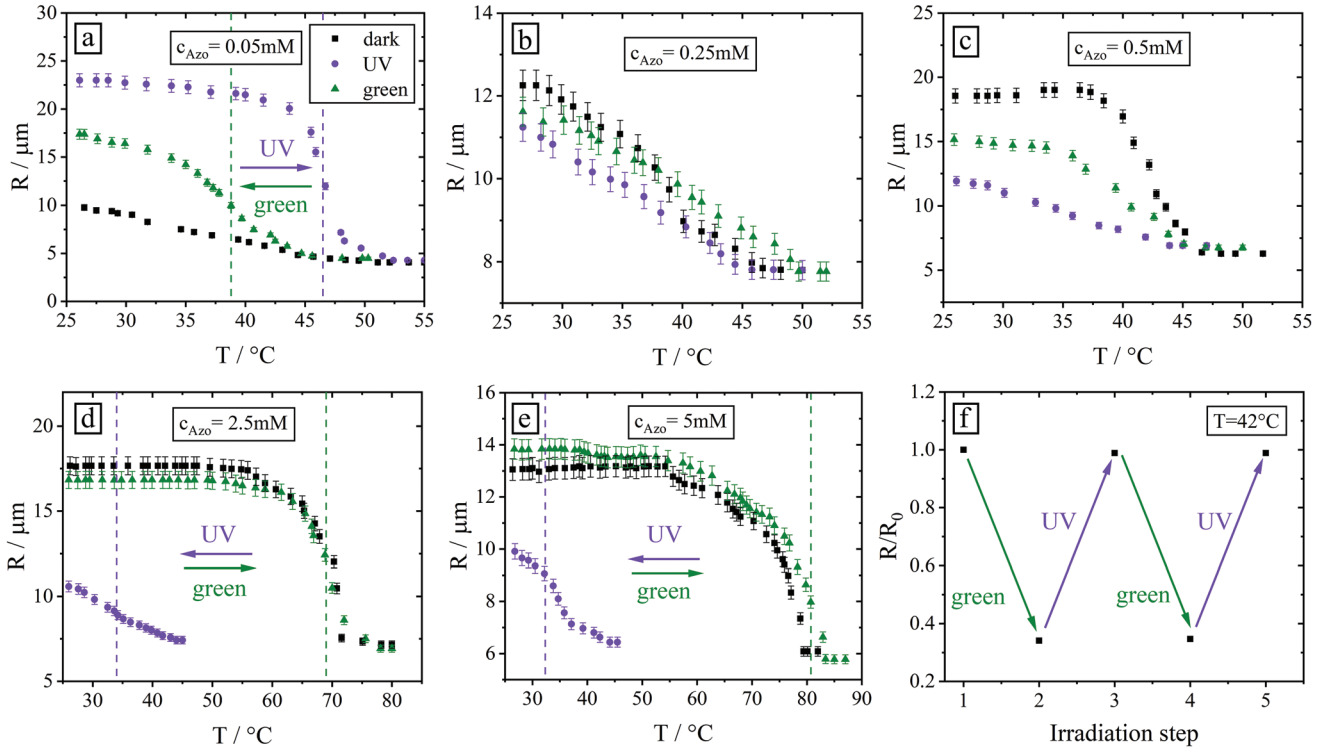

Figure 6. Switching of the particle radius by temperature and light for the 10 mol% AAc microgel dispersed in surfactant solution of different concentration: a) $c_{azo} = 0.05$ mM (Region I), b) $c_{azo} = 0.25$ mM (intersection of Regions I and II), c) $c_{azo} = 0.5$ mM (Region II), d) $c_{azo} = 2.5$ mM (Region II), e) $c_{azo} = 5$ mM (Region II). f) The change in the radius of the microgel from a) at fixed $T = 42$ °C. The corresponding video is provided in Integrated Multimedia.

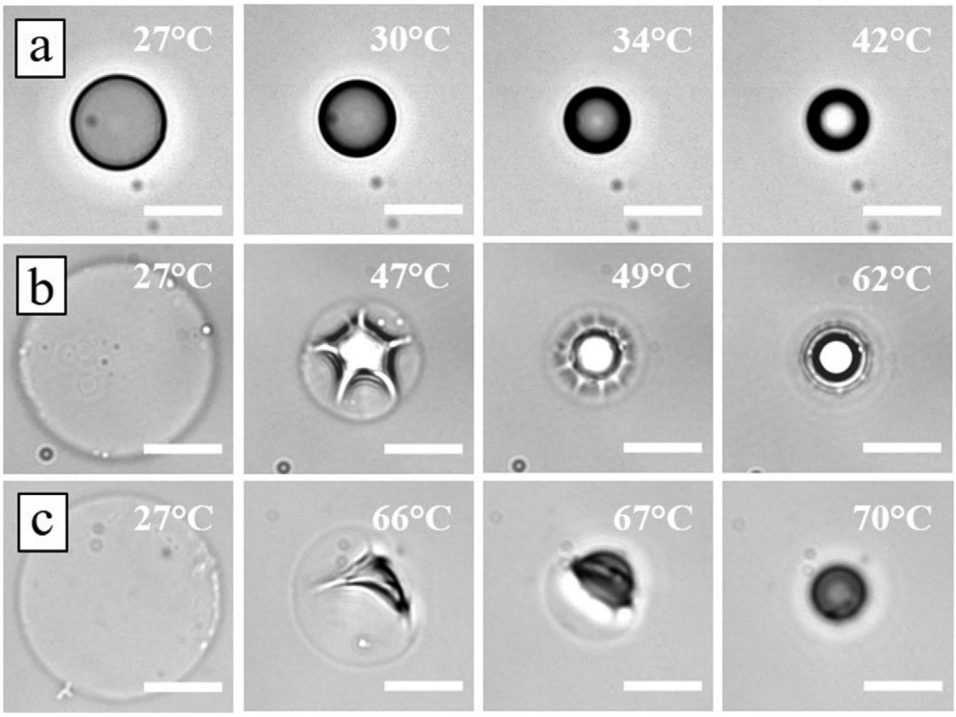

Figure 7. Examples of different shape change of microgel particles under varying temperature and irradiation wavelength. a) Microgel with 5 mol% AAc in 0.5 mM surfactant aqueous solution in dark, b) microgel with 10 mol% AAc in 0.05 mM surfactant aqueous solution under UV irradiation (see Figure 6a). c) 20 mol% AAc microgel in water (no added surfactant) in dark. The scale bar is 20 µm. The corresponding videos are provided in Integrated Multimedia.

and for strongly charged gels (10 and 20 mol%) even exceeds it by several degrees (for example for 10 mol% in water T_{VPTT} = 62 °C, while in 10 mM surfactant solution T_{VPTT} = 82 °C). Due to photo-sensitivity of the added surfactant, the VPTT point can be reversible shifted by light, since under irradiation the surfactant photo-isomerizes and either leaves (*cis*-state) or accommodate (*trans*-state) within the particle. The change of the VPTT is reversible and can be as high as 50 °C (for 10 mol% AAc gel in 10 mM surfactant concentration). Additionally, the peculiarity of the system is that at any chosen temperature (in the range between ≈32 °C and ≈60 °C) one can switch the size of the particle by irradiating it with light of appropriate wavelength. This opens manifold applications, for instance, in body care since at physiological temperature of 37 °C the microgel radius can be reversible switched within few seconds of irradiation in 3 times, that is, between 7 and 21 μm.

Supporting Information

Supporting Information is available from the Wiley Online Library or from the author.

Acknowledgements

This research is supported by DFG project (SA1572/17-1) and the Helmholtz Graduate School on Macromolecular Bioscience (Teltow, Germany). Authors thank SFB 985 "Functional Microgels and Microgel Systems" for financial support of this work. E.Y.K. and Y.D.G. are grateful to the Ministry of Science and Higher Education of the Russian Federation for financial support of the theoretical study (Agreement No. 075-15-2021-622). Access to electronic scientific resources for theoretical research was provided by Lomonosov Moscow State University and INEOS RAS with the support of the Ministry of Science and Higher Education of the Russian Federation.

Open access funding enabled and organized by Projekt DEAL.

Conflict of Interest

The authors declare no conflict of interest.

Data Availability Statement

Research data are not shared.

Keywords

azobenzene-containing surfactants, microgels, photo-responsive microgels, volume phase transition temperature point

Received: August 10, 2021
Revised: September 3, 2021
Published online:

[1] M. Karg, A. Pich, T. Hellweg, T. Hoare, L. A. Lyon, J. J. Crassous, D. Suzuki, R. A. Gumerov, S. Schneider, I. I. Potemkin, W. Richtering, *Langmuir* **2019**, *35*, 6231.
[2] Y. Hertle, T. Hellweg, *J. Mater. Chem. B* **2013**, *1*, 5874.
[3] J. Oberdisse, T. Hellweg, *Colloid Polym. Sci.* **2020**, *298*, 921.
[4] F. A. Plamper, W. Richtering, *Acc. Chem. Res.* **2017**, *50*, 131.
[5] W. Richtering, I. I. Potemkin, A. A. Rudov, G. Sellge, C. Trautwein, *Nanomedicine* **2016**, *11*, 2879.
[6] A. A. Polotsky, F. A. Plamper, O. V. Borisov, *Macromolecules* **2013**, *46*, 8702.
[7] M. Kather, M. Skischus, P. Kandt, A. Pich, G. Conrads, S. Neuss, *Angew. Chem., Int. Ed.* **2017**, *56*, 2497.
[8] Y. Wang, J. S. Nie, B. S. Chang, Y. F. Sun, W. L. Yang, *Biomacromolecules* **2013**, *14*, 3034.
[9] A. Barry, B. DeForest, A. C. DeForest, *Annu. Rev. Biomed. Eng.* **2019**, *21*, 241.
[10] D. Lu, M. Zhu, W. Wang, S. Wu, B. R. Saunders, D. J. Adlam, J. A. Hoyland, C. Hofzumahaus, S. Schneider, K. Landfester, *Soft Matter* **2019**, *15*, 527.
[11] K. Gawlitza, S. T. Turner, F. Polzer, S. Wellert, M. Karg, P. Mulvaney, R. von Klitzing, *Phys. Chem. Chem. Phys.* **2013**, *15*, 15623.
[12] M. Wiese, O. Nir, D. Wypysek, L. Pokern, M. Wessling, *J. Membr. Sci.* **2019**, *569*, 7.
[13] M. Wolff, H. J. M. Kather, H. Breisig, W. Richtering, A. Pich, M. Wessling, *ACS Appl. Mater. Interfaces* **2018**, *10*, 24799.
[14] R. H Pelton, P. Chibante, *Colloids Surf.* **1986**, *20*, 247.
[15] M. Heskins, J. E. Guillet, *J. Macromol. Sci. A* **1968**, *2*, 37.
[16] Y. Hirokawa, T. Tanaka, *J. Chem. Phys.* **1985**, *81*, 6379.
[17] K. Haruma, *Gels* **2020**, *6*, 26.
[18] H. G. Schild, D. A. Tirrell, *J. Phys. Chem.* **1990**, *94*, 4352.
[19] F. M. Winnik, *Macromolecules* **1990**, *23*, 233.
[20] A. Halperin, M. Kroger, F. M. Winnik, *Angew. Chem., Int. Ed.* **2015**, *54*, 15342.
[21] Y. K. Kim, E.-J. Kim, J. H. Lim, H. K. Cho, W. J. Hong, H. H. Jeon, B. G. Chung, *Nanoscale Res. Lett.* **2019**, *14*, 77.
[22] L. Tang, L. Wang, X. Yang, Y. Feng, Y. Li, W. Feng, *Prog. Mater. Sci.* **2021**, *115*, 100702.
[23] A. Burmistrova, R. von Klitzing, *J. Mater. Chem.* **2010**, *20*, 3502.
[24] X. Liu, H. Guo, L. Zha, *Polym. Int.* **2012**, *61*, 1144.
[25] L. W. Xia, X. J. Ju, J. J. Liu, R. Xie, L. Y. Chu, *J. Colloid Interface Sci.* **2010**, *349*, 106.
[26] R. Begum, Z. H. Farooqi, S. R. Khan, *Int. J. Polym. Mater. Polym. Biomater.* **2016**, *65*, 841.
[27] G. Agrawal, R. Agrawal, *Small* **2018**, *14*, 1801724.
[28] C. Hofzumahaus, P. Hebbeker, S. Schneider, *Soft Matter* **2018**, *14*, 4087.
[29] K. Kratz, Th. Hellweg, W. Eimer, *Colloids Surf., A* **2000**, *170*, 137.
[30] N. Seddiki, D. B. Aliouche, *Chem. Soc. Ethiopia* **2013**, *27*, 447.
[31] M. H. Kwok, Z. Li, T. Ngai, *Langmuir* **2013**, *29*, 9581.
[32] F. Monti, S.-Y. Fu, I. Iliopoulos, M. Cloitre, *Langmuir* **2008**, *24*, 11474.
[33] T. Wan, M. Xu, L. Y. Chen, D. Q. Wu, W. Z. Cheng, R. X. Li, C. Z. Zou, *J. Chem. Sci.* **2014**, *126*, 1623.
[34] J. Zhang, L.-Y. Chu, Ch.-J. Cheng, D.-F. Mi, M.-Y. Zhou, X.-Y. Ju, *Polymer* **2008**, *49*, 2595.
[35] Y. Zakrevskyy, M. Richter, S. Zakrevska, N. Lomadze, R. Klitzing, S. Santer, *Adv. Funct. Mater.* **2012**, *22*, 5000.
[36] S. Schimka, N. Lomadze, M. Rabe, A. Kopyshev, M. Lehmann, R. von Klitzing, A. M. Rumyantsev, E. Kramarenko, S. Santer, *Phys. Chem. Chem. Phys.* **2017**, *19*, 108.
[37] S. Schimka, Y. D. Gordievskaya, N. Lomadze, M. Lehmann, R. von Klitzing, A. M. Rumyantsev, E. Kramarenko, S. Santer, *J. Chem. Phys.* **2017**, *147*, 031101.
[38] A. M. Rumyantsev, S. Santer, E. Y. Kramarenko, *Macromolecules* **2014**, *47*, 5388.
[39] S. Santer, *J. Phys. D: Appl. Phys.* **2017**, *51*, 013002.
[40] A. L. M. Le Ny, C. T. Lee, *Biophys. Chem.* **2009**, *142*, 76.
[41] A. Diguet, N. K. Mani, M. Geoffroy, M. Sollogoub, D. Baigl, *Chem. - Eur. J.* **2010**, *16*, 11890.

[42] A. Zinchenko, *Adv. Colloid Interface Sci.* **2016**, *232*, 70.
[43] S. Rudiuk, K. Yoshikawa, D. Baigl, *Soft Matter* **2011**, *7*, 5854.
[44] A. A. Zinchenko, M. Tanahashi, S. Murata, *ChemBioChem* **2012**, *13*, 105.
[45] A. Kopyshev, K. Kanevche, N. Lomadze, E. Pfitzner, S. Loebner, R. R. Patil, J. Genzer, J. Heberle, S. Santer, *ACS Appl. Polym. Mater.* **2019**, *1*, 3017.
[46] A. Kopyshev, N. Lomadze, D. Feldmann, J. Genzer, S. Santer, *Polymer* **2015**, *79*, 65.
[47] A. Kopyshev, C. J. Galvin, R. R. Patil, J. Genzer, N. Lomadze, D. Feldmann, J. Zakrevski, S. Santer, *ACS Appl. Mater. Interfaces* **2016**, *8*, 19175.
[48] A. Venancio-Marques, F. Barbaud, D. Baigl, *J. Am. Chem. Soc.* **2013**, *135*, 3218.
[49] P. Arya, J. Jelken, D. Feldmann, N. Lomadze, S. Santer, *J. Chem. Phys.* **2020**, *152*, 194703.
[50] D. Feldmann, P. Arya, TY. Molotilin, N. Lomadze, A. Kopyshev, O. I. Vinogradova, S. Santer, *Langmuir* **2020**, *36*, 6994.
[51] P. Arya, D. Feldmann, A. Kopyshev, N. Lomadze, S. Santer, *Soft Matter* **2020**, *16*, 1148.
[52] E. Chevallier, A. Mamane, H. A. Stone, C. Tribet, F. Lequeux, C. Monteux, *Soft Matter* **2011**, *7*, 7866.
[53] L. Nurdin, A. Venancio-Marques, S. Rudiuk, M. Morel, D. Baigl, *C. R. Chim.* **2016**, *19*, 199.
[54] M. Schmitt, H. Stark, *Phys. Fluids* **2016**, *28*, 012106.
[55] N. Kavokine, M. Anyfantakis, M. Morel, S. Rudiuk, T. Bickel, D. Baigl, *Angew. Chem., Int. Ed.* **2016**, *55*, 11183.
[56] M. Anyfantakis, D. Baigl, *Angew. Chem., Int. Ed.* **2014**, *53*, 14077.
[57] S. N. Varanakkottu, S. D. George, T. Baier, S. Hardt, M. Ewald, M. Biesalski, *Angew. Chem., Int. Ed. Engl.* **2013**, *52*, 7291.
[58] A. Diguet, H. Li, N. Queyriaux, Y. Chen, D. Baigl, *Lab Chip* **2011**, *11*, 2666.
[59] D. Baigl, *Lab Chip* **2012**, *12*, 3637.
[60] R. Walter, J. Ricˇka, Ch. Quellet, R. Nyffenegger, Th. Binkert, *Macromolecules* **1996**, *29*, 4019.
[61] H. G. Schild, D. A. Tirrell, *Langmuir* **1991**, *7*, 665.
[62] J. Ricka, M. Meewes, R. Nyffenegger, Binkert Th, *Phys. Rev. Lett.* **1990**, *65*, 657.
[63] P. Arya, J. Jelken, N. Lomadze, S. Santer, M. Bekir, *J. Chem. Phys.* **2020**, *152*, 2.
[64] A. R. Khokhlov, E. Y. Kramarenko, E. E. Makhaeva, S. G. Starodubtzev, *Theory. Theory Simul.* **1992**, *1*, 105.
[65] V. Baulin, E. Y. Kramarenko, A. R. Khokhlov, *Comput. Theor. Polym. Sci.* **2000**, *10*, 165.